

The Critical Regime of the Metal-Insulator Transition in Conducting Polymers:

Experimental Studies

Alan J. Heeger

Department of Physics

and

Institute for Polymers and Organic Solids

University of California at Santa Barbara,

Santa Barbara, CA 93106

Abstract

The metal-insulator (M-I) transition in conducting polymers is particularly interesting; critical behavior has been observed over a relatively wide temperature range in a number of systems, including polyacetylene, polypyrrole, poly(phenylene vinylene) and polyaniline. In each case, metallic, critical and insulating regimes have been identified through Zhabrofskii plots of the logarithmic derivative of the conductivity. The critical regime (in which the conductivity varies as T^β , where $\beta \approx 1/3$) is tunable by varying the extent of disorder and by applying external pressure and/or an external magnetic field. The transitions from metallic to critical behavior and from critical to insulating behavior have been induced with a magnetic field and from insulating to metallic behavior with applied pressure.

Key words: Metal-insulator transition, disorder, conducting polymers

1. Introduction

Ioffe and Regel¹ argued that as the extent of disorder increased in a metallic system, there was a limit to metallic behavior; when the mean free path becomes less than the inter-atomic spacing, coherent metallic transport would not be possible. Thus, the Ioffe-Regel criterion is defined as

$$k_F l \sim 1, \quad (1)$$

where k_F is the Fermi wave number and l is the mean free path. The metallic regime corresponds to $k_F l \gg 1$. Based on the Ioffe-Regel criterion, Mott proposed^{2,3} that a metal-insulator (M-I) transition must occur when the disorder is sufficiently large that $k_F l < 1$. In recognition of Anderson's early work on disorder induced localization, Mott called this M-I transition the "Anderson transition".⁴ In the limit where $k_F l \ll 1$ (i.e. where the strength of the random disorder potential is large compared to the bandwidth), all states become localized and the conductor becomes a "Fermi glass";⁵ i.e. a continuous density of localized states occupied according to Fermi statistics. Although there is no energy gap in a Fermi glass, the behavior is that of an insulator because the states at the Fermi energy are spatially localized.

Mott pointed out that the states in band tails are more susceptible to localization.^{2,3} Consequently, there exists a critical energy separating the localized states from the delocalized states, called the mobility edge (E_c). For a specific "metallic" system with a

fixed number of electrons, the mobility edge approaches the Fermi energy as $k_F l$ decreases. When the Fermi energy falls on the side of E_c where the states are localized, the system undergoes a transition from a metal to a Fermi glass insulator. The scaling theory of localization demonstrated that the disorder-induced M-I transition was a true phase transition with a well defined critical point.⁶ MacMillan⁷ and later Larkin and Khmel'nitskii,⁸ showed that near the critical regime of Anderson localization, a power law temperature dependence is to be expected for the electrical conductivity,

The M-I transition in conducting polymers is particularly interesting; critical behavior has been observed over a relatively wide temperature range in a number of systems, including polyacetylene, polypyrrole, poly(p-phenylene vinylene), and polyaniline.⁹ In each case, the metallic, critical and insulating regimes near the M-I transition have been identified from Zabrodskii plots of the logarithmic derivative of the conductivity $W = (\Delta \ln \sigma / \Delta \ln T)$ vs T .¹⁰ In the metallic and insulating regime $W(T)$ exhibits positive and negative temperature coefficients, respectively, while in the critical regime, $W(T)$ is temperature independent.

The resistivity, $\rho(T)$, and the resistivity ratio, $\rho_r = \rho(1.4 \text{ K}) / \rho(300 \text{ K})$, have been successfully used to quantify the relative disorder in different samples and for sorting out the various regimes.^{9,11-14} In general, the resistivity at room temperature increases as the disorder increases. In addition, $\rho(T)$ increases more rapidly upon lowering the

temperature; i.e. ρ_r increases. In fact, the resistivity ratio (ρ_r) has proven to be useful as an "effective order parameter" for the metal-insulator (M-I) transition in conducting polymers.^{9,14}

2. The Critical regime and Crossover to the Metallic and Insulating Regimes

In conducting polymers, the critical regime is easily tunable by varying the extent of disorder (i.e. by studying samples with different ρ_r), or by applying external pressure and/or magnetic fields. The transitions from metallic to critical behavior and from critical to insulating behavior have been induced with a magnetic field, and from insulating to critical and then to metallic behavior with increasing external pressure.⁹

In the metallic regime, the zero temperature conductivity remains finite, and $\sigma(T)$ can be expressed as follows:

$$\sigma(T) = \sigma_0 + f(T), \quad (2)$$

where $f(T)$ is mainly determined by the electron-electron interaction and localization contributions to the conductivity.^{9,11-14} The magnitude of σ_0 depends on the extent of the disorder. Metallic behavior has been demonstrated for conducting polymers with $\sigma(T)$ remaining constant as T approaches zero.⁹ Well into the metallic regime where the mean free path extends over many repeat units, σ_0 is quite large, approaching that of a metal.

However, the true metallic regime, with $k_F l \gg 1$ such that $\rho(T)$ decreases as the temperature is lowered has not yet been achieved.

In the critical region, theory predicts that the resistivity should follow the power law^{7,8}

$$\rho(T) \approx (4\pi^2 e^2 p_F / h^2) (k_B T / E_F)^{-1/\eta} = AT^\beta; \quad (3)$$

where p_F is the Fermi momentum, h is Planck's constant, and e is the electron charge. A value of $\beta \approx 1/3$ indicates that the system is just on the metallic side of the M-I transition. Extension of the power law dependence all the way to $T = 0$ requires that the system be *precisely* at the critical point. The power law is universal and requires only that the disordered system be in the critical regime.

The power law dependence for $\sigma(T)$ has been observed over a wide temperature range in a number of "metallic" polymers near the M-I transition; the results are in good quantitative agreement with Eqn 3.^{9,11-14} Log-log plots of $W(T) = (\Delta \ln \sigma / \Delta \ln T)$ vs T are quite sensitive and enable the precise identification of the critical regime.¹⁵ Moreover, the detailed evolution of $\sigma(T)$ in the critical regime at low temperatures can be observed in $W(T)$ plots as the system is changed from metal to insulator (by changing the extent of the disorder or by tuning with pressure or magnetic field). Although $W(T)$ is temperature independent for a wide range of temperatures below 50K, β systematically increases from

values less than 1/3 (on the metallic side) toward 1 as the system is moved toward the insulating side.¹⁵

In the insulating regime, transport occurs through variable range hopping (VRH) among localized states. For Mott VRH conduction (noninteracting carriers) in three dimensions^{2,3}

$$\ln \rho \propto (T_0/T)^{1/4}, \quad (4a)$$

where

$$T_0 = 18/k_B L_v^3 N(E_F), \quad (4b)$$

k_B is the Boltzmann constant, L_v is the localization length, and $N(E_F)$ is the density of states at the Fermi energy. In one-dimension and in two dimensions, the exponent is 1/2 and 1/3, respectively. When the Coulomb interaction between the electron which is hopping and the hole left behind is dominant,¹⁶

$$\ln \rho \propto (T_0'/T)^{1/2}, \quad (5a)$$

where

$$T_0' = \beta_I e^2 / \epsilon k_B L_v, \quad (5b)$$

e is the electron charge, ϵ is the dielectric constant, and $\beta_I = 2.8$ (a numerical constant).

Thus, in general, in the insulating regime, $\ln \rho$ is proportional to $T^{-1/x}$ where x is determined by details of the phonon-assisted hopping.

The temperature dependences of $W(T)$ in various regimes near the M-I transition are as follows:

- (a) In the metallic regime, W has a positive temperature coefficient.
- (b) In the critical regime, W is temperature independent for a wide range of temperatures.
- (c) In the insulating regime, W has a negative temperature coefficient.

Fig. 1 shows a schematic diagram of the electrical conductivity vs temperature in the vicinity of the metal-insulator transition. Each of the curves shown in Fig.1 is drawn for a different degree of disorder; for a given conducting polymer system, each curve would represent data obtained from a sample with different resistivity ratio, ρ_r .

Precisely at the critical point (where the mobility edge is precisely at the Fermi energy), the conductivity follows the power law of Eqn 3. On the metallic side, the conductivity remains finite as the temperature approaches zero as indicated in Eqn 2. On the insulating side, the conductivity falls below the power law as a result of the exponential dependence that results from variable range hopping; see Eqn 4 and 5. Near, but not precisely at, the critical point, the resistivity follows the power law dependence over a restricted range of temperatures. Toward the metallic side of the M-I transition, the exponent of the power law is less than $1/3$ (values as small as 0.1 have been observed);¹⁵ toward the insulating side of the M-I transition, the exponent of the power law is greater than $1/3$ (values as large as 1 have been observed). As shown in Fig. 1, however, at

sufficiently low temperatures, the power law dependence is maintained only at the critical point.

Application of a large magnetic field tends to localize the electrons; the magnetic field shifts the Fermi energy toward the mobility edge.^{17,18} Thus, in Fig. 1, increasing the magnetic field tends to cause a trajectory from the metallic side toward the insulating side. A magnetic field induced crossover from the critical regime (power law dependence) to the insulating regime (variable range hopping) has been demonstrated for polyaniline.¹⁷ Application of high pressure increases the interchain interaction making interchain hopping more facile. High pressure, therefore, inhibits localization. A pressure induced crossover from the critical regime (power law dependence) to the metallic regime has also been demonstrated.⁹

The magnetic field – induced crossover from the critical regime (with $\rho(T) = AT^\beta$) to the insulating regime (with $\ln\rho \propto (T_0/T)^{1/4}$) is shown in Fig. 2 for polyaniline doped with camphor-sulfonic acid (PANI – CSA) (see ref. 11).

3. Infrared Reflectance Studies of the Metallic State and the M-I Transition

Reflectance measurements provide information on the electronic structure over a wide spectral range; measurements in the infrared (IR) probe the intraband (free carrier) excitations, while measurements at higher photon energies probe the interband transitions. The corresponding optical/IR conductivity, $\sigma(\omega)$, provides information on the

metal physics the disorder-induced metal-insulator transition, and the joint density of states associated with interband transitions at higher energies. Not surprisingly, IR reflectance measurements have played an important role in clarifying the metal physics of conducting polymers.

In spite of the evidence for the disorder-induced M-I transition as inferred from the transport⁹ and optical measurements,^{19,20} the metallic state of conjugated polymers has been a subject of controversy. Although disorder is generally recognized to play an important role in the physics of “metallic” polymers, the effective length scale of the disorder and the nature of the M-I transition are the central unresolved issues.^{21,22} In particular, the question of whether disorder is present over a wide range of length scales or whether the properties are dominated by more macroscopic inhomogeneities has been a subject of discussion. In the former case, the metallic state and the M-I transition could be described by conventional localization physics (e.g. the Anderson transition), while in the latter case, the M-I transition would be better described in terms of percolation between metallic islands.²¹

Recent progress in the processing of conducting polymers has significantly improved the quality of the materials and reduced the extent of structural disorder with corresponding improvements in the electrical conductivity. Examples of such improved materials include polyaniline and polypyrrole doped with PF₆, PPy-PF₆.⁹ Extensive

transport studies on PPy-PF₆²³ demonstrated that the improved material is more highly conducting and more homogeneous than that studied earlier.²⁴

As is typical of conducting polymers, PPy-PF₆ is partially crystalline. The structural coherence length is, however, only $\xi \approx 20\text{-}50 \text{ \AA}$, less than any length used to characterize the electronic properties, i.e. less than the inelastic scattering length ($L_{in} \approx 300 \text{ \AA}$) in the metallic regime, and less than the localization length ($L_c \approx 200\text{-}300 \text{ \AA}$) in the insulating regime near the M-I transition.^{9,23} Moreover, the corresponding transport data in the critical regime and the crossover from metal to insulator have been successfully analyzed in terms of conventional disorder-induced localization.^{9,23}

Kohlman *et al.*^{22,25,26} reported infrared reflectance measurements, $R(\omega)$, which they analyzed in terms of the frequency dependent optical constants. They reported a zero-crossing in the dielectric function, $\epsilon_1(\omega)$, at $\omega \approx 250 \text{ cm}^{-1}$ (well below the π -electron plasma frequency at 1.2 eV). At frequencies below the zero-crossing, they reported $\epsilon_1(\omega)$ becoming increasingly negative. This low frequency zero-crossing is not consistent with a disordered metal near the M-I transition; they attributed the zero crossing to a plasma resonance associated with a low density of 'delocalized carriers' with an anomalously long scattering time ($t \approx 10^{-11} \text{ sec}$).^{22,25,26} Metallic PPy-PF₆ was therefore described as inhomogeneous, consisting of a composite of metallic islands (crystalline regions) embedded in an amorphous matrix. From this point of view, the M-I transition was

interpreted in terms of percolation between the metallic islands.^{22,25,26} The inference of a small fraction of carriers with long relaxation time was used to predict ultra-high conductivity polymers in which all the carriers were delocalized with similarly long scattering times.^{22,25,26}

To clarify the nature of the metallic state, high precision reflectance measurements were carried out over a wide spectral range on a series of PPy-PF₆ samples in the insulating, critical, and metallic regimes near the M-I transition.²⁷ Since the reflectance in the infrared (IR) is sensitive to the charge dynamics of carriers near the Fermi energy (E_F), such a systematic reflectance study can provide information on the electronic states near E_F and how those states evolve as the system passes through the M-I transition. The data demonstrate that metallic PPy-PF₆ is a 'disordered metal' and that the M-I transition is driven by disorder; similar results were obtained for polyaniline.^{20,28} The data showed no evidence of a zero-crossing in $\epsilon_1(\omega)$ at frequencies as low as $\omega = 8 \text{ cm}^{-1}$, even for the most metallic samples. The absence of the low frequency zero crossing implies that the small fraction of 'delocalized carriers' with anomalously long scattering time does not exist.

Free-standing films of PPy-PF₆ were prepared by electrochemical polymerization.²³ Although the preparation conditions are more or less identical for all samples, details of the synthesis and processing lead to subtle changes in the sample quality, and thereby to

changes in the electrical properties. Therefore, each of the samples was fully characterized by performing complete transport measurements (as noted in the Introduction) ρ_r can be used as an effective order parameter to characterize the strength of the disorder). Based on the criteria summarized in the Introduction, sample A ($\rho_r = 1.7$) is in the metallic regime, and sample F ($\rho_r = 160$) is in the insulating regime. For samples B ($\rho_r = 2.5$), C ($\rho_r = 2.8$), D ($\rho_r = 6.0$), D ($\rho_r = 7.8$) and E ($\rho_r = 7.8$), the electronic properties gradually evolve from the metallic side of the M-I transition to the insulating side via the critical regime. Thicknesses of the free standing films were typically 10-20 μm .

Since even a few percent error in $R(\omega)$ is crucial to the Kramers-Kronig (K-K) analysis, extra care was taken in all procedures for obtaining absolute values for $R(\omega)$. Surface quality is essential for accurate reflectance measurements. Therefore, the surface morphology of each film was checked, both optically and using scanning electron microscopy.²⁹ All the sample surfaces were of excellent optical quality and exhibited specular reflection. Thus, any scattering loss contribution to the measured IR reflectance was negligible. A gold mirror ($R = 1$ in the IR) was used for reference. The systematic error in the $R(\omega)$ measurements was estimated to be within 1%.

Fig. 3 shows $R(\omega)$ for samples (A-F) as measured at room temperature. For the most metallic sample (A), $R(\omega)$ exhibits distinct metal-like signatures; a free carrier plasma

resonance as indicated by the minimum in $R(\omega)$ around $1.5 \times 10^4 \text{ cm}^{-1}$ and high $R(\omega)$ in the far-IR ($R \approx 90\%$ for $\omega < 20 \text{ cm}^{-1}$). As PPy-PF₆ goes from the metallic to the insulating regime via the critical regime (Samples A through F), $R(\omega)$ is gradually suppressed in the IR. In the insulating regime (F), $R(\omega)$ remains well below that of the metallic sample (A) throughout the IR ($R \approx 65\%$ at $\omega = 50 \text{ cm}^{-1}$). Note that the $R(\omega)$ spectra are in excellent correspondence with the transport results (this is especially clear at low frequencies in Fig. 2); the better the quality of the sample, as defined by smaller ρ_r and higher $\sigma_{dc}(300\text{K})$, the higher $R(\omega)$ in the IR.

In the far-IR (below 100 cm^{-1}), the Hagen-Rubens (H-R) approximation provides an excellent fit to $R(\omega)$,

$$R_{\text{H-R}}(\omega) = 1 - (2\omega/\pi\sigma_{\text{H-R}})^{1/2}, \quad (6)$$

where $\sigma_{\text{H-R}}$ is the ω -independent conductivity. The $\sigma_{\text{H-R}}$ values obtained from the Hagen-Rubens fits are in remarkably good agreement with the measured values of $\sigma_{dc}(300\text{K})$. The excellent fits and the agreement between $\sigma_{\text{H-R}}$ and $\sigma_{dc}(300\text{K})$ imply a weak ω -dependence in the corresponding optical conductivity, $\sigma(\omega)$, for $\omega < 100 \text{ cm}^{-1}$.

For each data set, the complex dielectric function, $\epsilon(\omega) = \epsilon_1(\omega) + i(4\pi/\omega)\sigma(\omega)$, was obtained by K-K analysis of $R(\omega)$. At the low frequency end, the H-R relation (Eqn. 6) was used to extrapolate to ω approaches 0.

The optical constants, $\sigma(\omega)$ and $\epsilon_1(\omega)$ are shown in Fig. 4. The corresponding $\sigma(\omega)$ are not typical of a Drude metal for which $\sigma_{\text{Drude}} = (\omega_p^2 \tau / 4\pi) / [1 + \omega^2 \tau^2]$, where ω_p is the π -electron plasma frequency, and τ is the mean scattering time. Even for the most metallic sample (A), $\sigma(\omega)$ decreases with decreasing ω below 2500 cm^{-1} and thus deviates from Drude behavior. On moving toward the insulating regime (from A to F), $\sigma(\omega)$ is suppressed, and the maximum in $\sigma(\omega)$ gradually shifts to higher frequencies. For all samples, however, there is a change in slope in $\sigma(\omega)$ at around $\omega \approx 100 \text{ cm}^{-1}$; at lower frequencies, $\sigma(\omega)$ is essentially frequency independent and, in each case, accurately approaches the measured $\sigma_{\text{dc}}(300\text{K})$ value. Indeed, such a weak ω -dependence for $\omega < 100 \text{ cm}^{-1}$ is expected from the excellent fit of $R(\omega)$ by the H-R approximation in this frequency range.

The dielectric function, $\epsilon_1(\omega)$, also deviates from the functional dependence expected for a Drude metal. Even for the highest conductivity and most metallic sample (A), $\epsilon_1(\omega)$ is positive in the IR, increasing to larger values for $\omega < 2500 \text{ cm}^{-1}$, and remaining positive at frequencies at least as low as $\omega = 8 \text{ cm}^{-1}$; see Fig. 4. The frequency-independent $\sigma(\omega)$ implies that $\epsilon_1(\omega)$ will remain positive as ω approaches 0; KK

consistency requires that for $\epsilon_1(\omega)$ to go negative below 8 cm^{-1} , $\sigma(\omega)$ would have to sharply increase as ω approaches zero. The excellent agreement between $\sigma(\omega)$ as ω approaches zero and $\sigma_{dc}(300\text{K})$, evident in the inset to Fig. 4 confirms the accuracy and precision of the $R(\omega)$ measurements and indicates that such an increase in $\sigma(\omega)$ as ω approaches 0 does not occur.

The positive dielectric function in the far-IR indicates that PPy-PF₆ is a ‘dirty’ metal with $\omega_p\tau \sim 1$; the overdamped plasma oscillation prevents the zero-crossing even at ω_p . In the critical (sample D) and insulating regimes (sample F), the overdamping of the plasma oscillation is even more clearly evident.

The ω -dependences of $\sigma(\omega)$ and $\epsilon_1(\omega)$ shown in Fig. 4 are not consistent with those reported by Kohlman et al.^{22,25,26} Based on reflectance measurements on PPy-PF₆ samples with transport properties comparable to those of sample A, a negative $\epsilon_1(\omega)$ with a zero-crossing around $\omega \approx 250 \text{ cm}^{-1}$ was reported. However, the corresponding $\sigma(\omega)$ inferred from their measurements extrapolates to $\sim 600 \text{ S/cm}$ as ω approaches zero, a value which is a factor of two larger than the measured σ_{dc} ($\approx 300 \text{ S/cm}$ at 300K). The negative $\epsilon_1(\omega)$ at low frequencies was attributed to the most delocalized electrons, and a Drude response with an unusually long τ ($\approx 10^{-11}$ sec) and mean free path ($l \sim 1 \mu\text{m}$) was inferred for a small fraction of the carriers. Such a long mean free path at room temperature has no precedent even in single crystals of pure metals such as copper and certainly not in

disordered materials where the crystalline coherence length is only 20-50 Å. Thus, an attempt to quantify the nature of the disorder in conducting polymers in terms of the percolation of weakly connected “metallic islands” via amorphous regions must be viewed with considerable skepticism.

Based upon Fig. 4, there is no zero-crossing in $\epsilon_1(\omega)$ down to $\omega \approx 50 \text{ cm}^{-1}$ even for the most metallic sample (with $\rho_r \approx 1.7 < 2$ and $\sigma_{dc}(300\text{K}) \approx 340 \text{ S/cm}$). The origin of the discrepancy might simply arise from small errors in the absolute value of the reflectance. The $\sigma(\omega)$ and $\epsilon_1(\omega)$ data shown in Figs. 4a and 4b do not exhibit the features of a two fluid model. Instead, in agreement with earlier work,^{28,30} the optical constants are fully consistent with the "localization-modified Drude model" (LMD). The suppressed $\sigma(\omega)$ and the increase in $\epsilon_1(\omega)$ as ω approaches 0 arise from weak localization induced by disorder. Moreover, the gradual evolution of $\sigma(\omega)$ from the insulating regime to the metallic regime implies that the M-I transition proceeds in the context of the Anderson transition. The $\sigma(\omega)$ data from the various regimes were fit with the functional dependence predicted by the LMD model:

$$\sigma_{LD}(\omega) = \sigma_{Drude} \{ 1 - C [1 - (3\tau\omega)^{1/2}] / (k_F l)^2 \}, \quad (7)$$

where in the insulating regime, $C=1$ and in the metallic regime, C is determined by the dc conductivity. In this model, the additional parameter, $k_F l$, is introduced in the first-order correction term.³¹ Fig. 5 illustrates the excellent agreement of the fits to the data with the

parameters summarized in the inset (except for the phonon features around 400 - 2000 cm^{-1} which are not included in the LMD model). There are small deviations for $\omega < 100 \text{ cm}^{-1}$ (more important in the less metallic samples), below which phonon-assisted hopping makes a measurable contribution to $\sigma(\omega)$ (and to the dc conductivity).

The parameters obtained from the fits are reasonable. The screened plasma frequency, $\Omega_p = \omega_p/(\epsilon_\infty)^{1/2} \approx 1.5 \times 10^4 \text{ cm}^{-1}$, is in good agreement with the frequency of the minimum in $R(\omega)$, and τ is typical of disordered metals ($\tau \approx 10^{-14} - 10^{-15} \text{ s}$). The quantity k_{Fl} is of particular interest for it characterizes the extent of disorder and is often considered as an order parameter in localization theory.^{31,32} For all four samples represented in Fig. 5, $k_{Fl} \approx 1$, implying that all are close to the M-I transition. As the disorder increases and the system moves from the metallic regime (sample A with $k_{Fl} = 1.38$) to the critical regime (sample E with $k_{Fl} = 1.01$), k_{Fl} approaches the Ioffe-Regel limit, precisely as would be expected. In the insulating regime (sample F) $k_{Fl} = 0.94 < 1$, consistent with localization of the electronic states at E_F .

4. Conclusion

The data obtained for metallic polymers indicate that they are 'disordered metals' near the disorder-induced M-I transition. The critical regime, and the metallic and insulating regimes near the critical regime, have been studied in detail. There is remarkable

consistency between the conclusions obtained from transport studies and from IR reflectance measurements.

References:

1. A.F. Ioffe and A.R. Regel, *Prog. Semicond.* **4**, 237 (1960).
2. N.F. Mott and E.A. Davis, *Electronic Processes in Noncrystalline Materials* (Oxford University Press, Oxford, 1979).
3. N.F. Mott, *Metal-Insulator Transition* (Taylor & Francis, London, 1990).
4. P.W. Anderson, *Phys. Rev.* **109**, 1492 (1958)
5. P.W. Anderson, *Comments on Sol. State Phys.*, **2**, 193 (1970).
6. E. Abrahams, P.W. Anderson, D.C. Licciardello and T.V. Ramakrishnan, *Phys. Rev. Lett.* **42**, 695 (1979).
7. W.L. McMillan, *Phys. Rev.* **B24**, 2739 (1981).
8. A.I. Larkin and D.E. Khmel'nitskii, *J. Exp. And Theoret. Phys.* **56**, 647 (1982).
9. R. Menon, C.O. Yoon, D. Moses and A.J. Heeger, *Handbook of Conducting Polymers*, 2nd Edition, Edited by T.A. Skotheim, R.L. Elsenbaumer and J.R. Reynolds, (Marcel Dekker, Inc. New Yor, 1998); p. 85.
10. A.G. Zabrodskii, and K.N. Zinovjeva, *Zh. Eksp. Teor. Fiz.* **86**, 727 (1984).
11. M. Reghu, C.O. Yoon, Y. Cao, D. Moses and A.J. Heeger, *Phys. Rev.* **B47**, 1758 (1993).

12. M. Reghu, K. Vakiparta, C.O. Yoon, Y. Cao, D. Moses and A.J. Heeger, *Synth. Met.* **65**, 167 (1994).
13. M. Reghu, K. Vakiparta, Y. Cao and D. Moses, *Phys. Rev.* **B49**, 16162 (1994).
14. R. Menon, D. Moses, and A.J. Heeger, *Phys. Rev.* **B49**, 10851 (1994).
15. M. Ahlskog, R. Menon and A.J. Heeger, *J. Phys.: Condensed Matter* **9**, 4145 (1997).
16. B.I. Shklovskii and A.L. Efros, *Electronic Processes in Doped Semiconductors* (Springer, Heidelberg, 1984).
17. R. Menon, Y. Cao, D. Moses and A.J. Heeger, *Phys. Rev.* **B47**, 1758 (1992).
18. D.E. Khmel'nitskii and A.I. Larkin, *Sol. State Commun.* **39**, 1069 (1981).
19. K. Lee, R. Menon, C.O. Yoon and A.J. Heeger, *Phys. Rev.* **B52**, 4770 (1995).
20. K. Lee, A.J. Heeger and Y. Cao, *Synth. Met.* **69**, 261 (1995).
21. R.S. Kohlman, J. Joo, and A.J. Epstein in *Physical Properties of Polymers Handbook*, Ed. By J. Mark (AIP, New York, 1996).
22. R.S. Kohlman, Joo, Y.Z. Wang, J.P. Pouget, H. Koneko, T. Ishiguro and A.J. Epstein, *Phys. Rev. Lett.* **74**, 773 (1995).
23. C. Yoon, M. Reghu, D. Moses, and A.J. Heeger, *Phys. Rev.* **B49**, 10851 (1994).
24. K. Sato, M. Yamamura, T. Hagiwara, K. Murata and M. Tokumoto, *Synth. Met.* **40**, 35 (1991).
25. R.S. Kohlman, A. Zibold, D.B. Tanner, G.G. Ihas, T. Ishiguro, Y.G. Min, A.G. MacDiarmid and A. Epstein, *Phys. Rev. Lett.* **78**, 3915 (1997).

26. A.J. Epstein, J.Joo, R.S. Kohlman, *Synth. Met.* **65**, 149 (1994).
27. K. Lee, E.K. Miller, A.N. Aleshin, R. Menon, A.J. Heeger, J.H. Kim, C.O. Yoon and H. Lee, *Adv. Mater.* **10**, 456 (1998).
28. K. Lee, A.J. Heeger and Y. Cao, *Phys. Rev. B* **48**, 14884 (1993).
29. J.H. Kim, H.K. Sung, C.O. Yoon and H. Lee, *Synth. Met.* **84**, 737 (1997).
30. K. Lee, A.J. Heeger and Y. Cao, *Synth. Met.* **72**, 25 (1995).
31. T.G. Castner in *Hopping Transport in Solids*, Ed. By M. Pollack and B.I. Shklovskii (Elsevier Science, Amsterdam, 1991).
32. P.A. Lee and T.V. Ramakrishnan, *Rev. Mod. Phys.* **57**, 287 (1985).

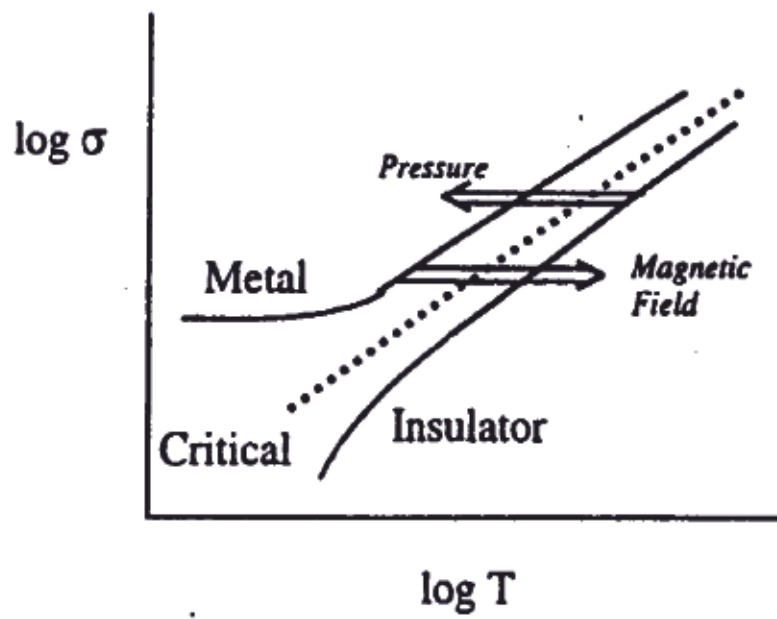


Figure 1: Schematic plot of $\text{Log } \sigma$ vs $\text{Log } T$ near the M-I transition. Application of a magnetic field can tune metallic samples across the M-I transition, and pressure can tune insulating samples across the transition. Along the critical line, $\sigma = T^p$.

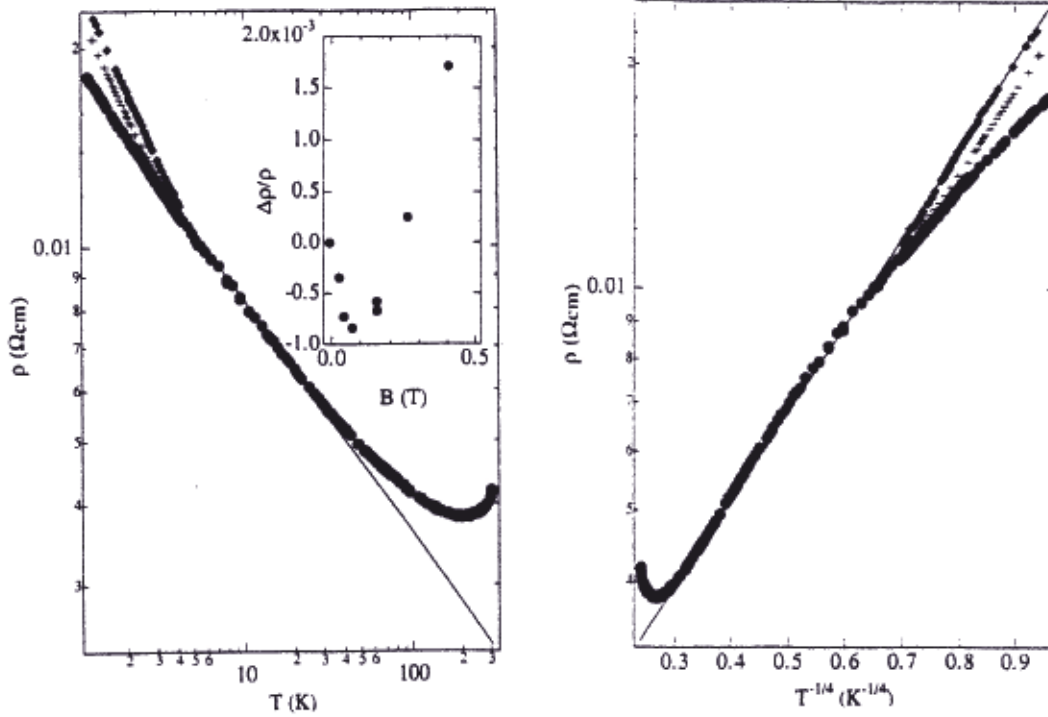
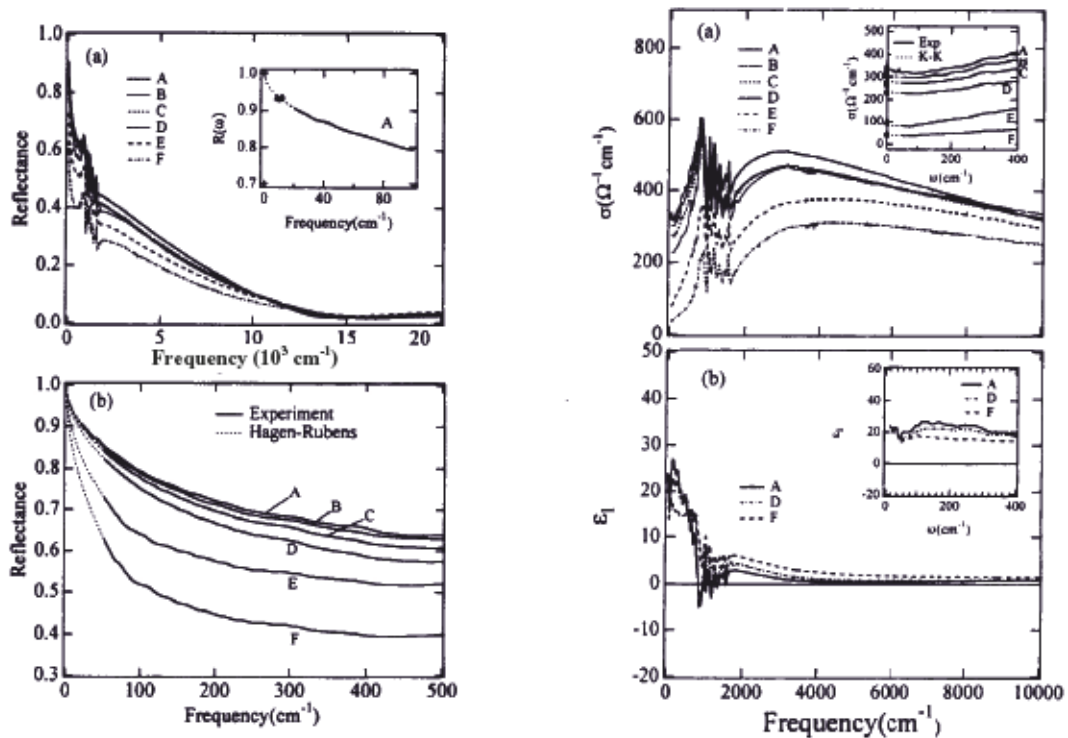


Figure 2: (Left) Log ρ vs log T for PANI-CSA; dots, $H = 0$, pluses, $H = 4\text{T}$, and diamonds, $H = 8\text{T}$. The solid line represents $\rho(T) \propto T^{-0.36}$. The inset shows the resistivity vs magnetic field at 1.2K . (Right) Log ρ vs $T^{-1/4}$ for PANI-CSA; dots, $H = 0$, pluses, $H = 4\text{T}$, and diamonds, $H = 8\text{T}$. The solid line represents VRH with $T_0 = 56\text{K}$.



(Left) Figure 3: $R(\omega)$ for Ppy-PF sample A-F at 300K. The inset shows $R(\omega)$ of the metallic sample, A, below 100 cm^{-1} ; the solid curve was obtained with a far-IR interferometer, the triangles were obtained with a sub-mm spectrometer, the dashed curve is the fit by the Hagen-Rubens formula with $\sigma = 310 \text{ S/cm}$.

(Right) Figure 4: $\sigma(\omega)$ and $\epsilon(\omega)$; the insets show the spectra in the far-IR. Note the excellent agreement between the dc conductivity and $\sigma(\omega)$ extrapolated to $\omega = 0$ from the K-K transform.

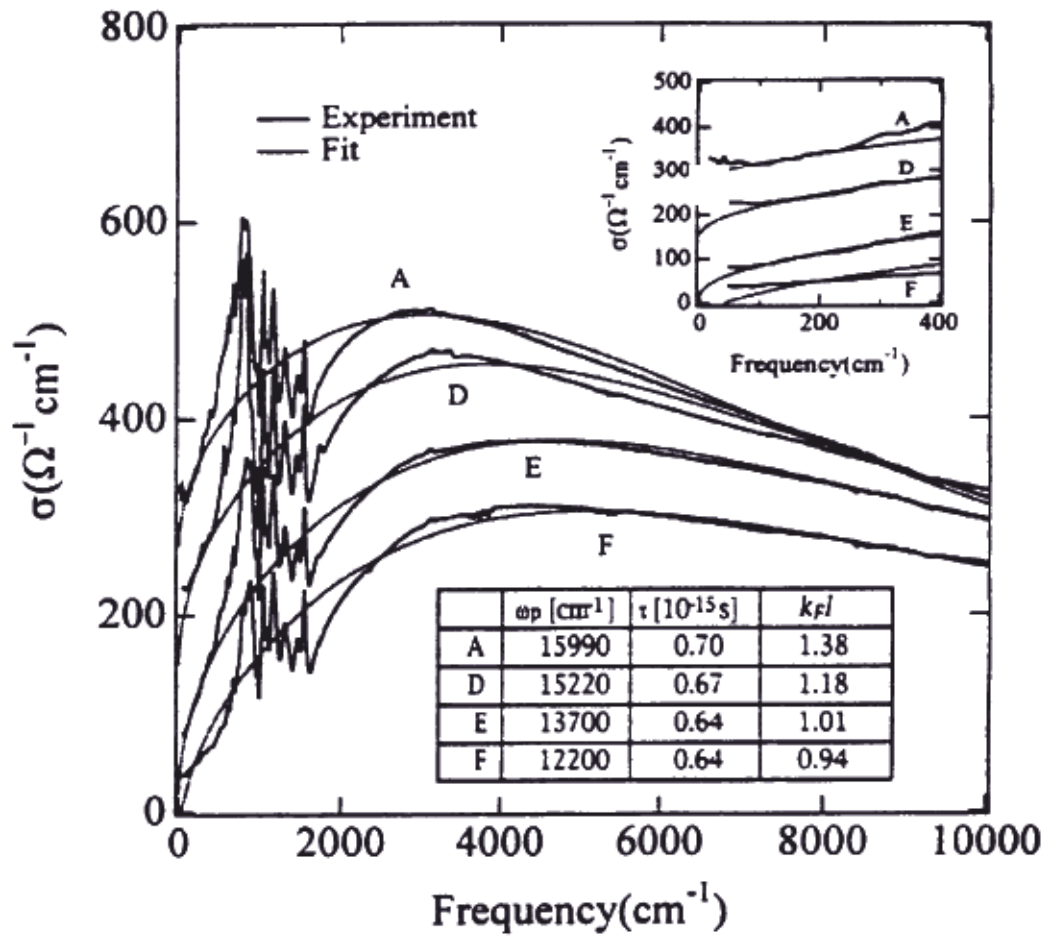


Figure 5: Comparison of the optical conductivity with the theoretical fit to the LMDmodel as described in the text, with the parameters shown in the inset. The spectra in the far-IR are shown in the second inset for more detailed comparison.